

Microwave-cut silicon layer transfer

D. C. Thompson, T. L. Alford,^{a)} and J. W. Mayer
*Department of Chemical and Materials Engineering, Arizona State University,
 Tempe, Arizona 85287-6006*

T. Hochbauer and M. Nastasi
*Materials Science and Technology Division, Los Alamos National Laboratory,
 Los Alamos, New Mexico 87544*

S. S. Lau
*Department of Electrical and Computer Engineering, University of California at San Diego,
 San Diego, California 92093*

N. David Theodore
*Advanced Products Research and Development Laboratory, Freescale Semiconductor Incorporated,
 2100 East Elliot Road, Tempe, Arizona 85284*

K. Henttinen and Ilkka Suni
VTT Centre for Microelectronics, P. O. Box 1208, 02044 VTT, Finland

Paul K. Chu
*Department of Physics and Materials Science, City University of Hong Kong, Tat Chee Avenue,
 Kowloon, Hong Kong*

(Received 21 July 2005; accepted 6 October 2005; published online 22 November 2005)

Microwave heating is used to initiate exfoliation of silicon layers in conjunction with the ion-cut process for transfer of silicon layers onto insulator or heterogeneous layered substrates. Samples were processed inside a 2.45 GHz, 1300 W cavity applicator microwave system for time durations as low as 12 s. This is a significant decrease in exfoliation incubation times. Sample temperatures measured by pyrometry were within previous published ranges. Rutherford backscattering spectrometry and cross-sectional transmission electron microscopy were used to determine layer thickness and crystallinity. Surface quality was measured by using atomic force microscopy. Hall measurements were used to characterize electrical properties as a function of postcut anneal time and temperature. © 2005 American Institute of Physics. [DOI: [10.1063/1.2135395](https://doi.org/10.1063/1.2135395)]

Ion-cut processes are becoming ever more mature and robust. At the same time, new and innovative ideas are being pursued for the use of ion-cut silicon-on-insulator (SOI) and heterostructures, with amazing success achieved in engineering solutions to fundamental problems in device architecture.^{1,2} In this work, the authors demonstrate a new innovation to the ion-cut process, namely the use of “microwave cutting”. The process involves inducing silicon exfoliation and layer transfer using microwave heating as a part of the ion-cut process. Microwaves have been paid a lot of recent attention for thermal synthesis, sintering, and joining of ceramic materials.^{3–5} Microwaves have even been used to initiate solid-state reactions in silicon.⁶ In the present work, microwaves are used as a means of reducing incubation time and heating power requirements, while attaining the temperatures needed for initiation of silicon exfoliation for the ion-cut process. Upon successful processing, samples are then characterized to explore damage, microroughness, crystallinity, and electrical behavior.

To fabricate the samples used in the ion-cut process Czochralski-grown *P*-type boron-doped 1–13 Ω cm (100) oriented silicon pieces were Radio Corporation of America RCA cleaned and placed in an Varion/Extrion Division 200-DF4 ion implanter where they were implanted with $0\text{--}3 \times 10^{15}/\text{cm}^2$, 175 keV B⁺ ions, and $9 \times 10^{16}/\text{cm}^2\text{--}1$

$\times 10^{17}/\text{cm}^2$, 50 keV H⁺, ions at room temperature. The implanted samples and nonimplanted silicon, coated with a chemically grown oxide, were then RCA cleaned and placed in a Tegal asher at 100 °C for plasma surface activation using a 300 W, 13.56 MHz, 0.3 SCFH oxygen rf plasma. After plasma activation, rinsing, and spin drying, the wafers were placed in surface-to-surface contact at room temperature. The bonded pairs were subsequently annealed in a mechanical furnace at 100 °C for 2 h to drive out any residual water at the bond interface.

After the furnace anneal, the bonded samples were placed in a 2.45 GHz 1300 W cavity applicator microwave system where they were processed for time durations ranging from 12 s to 1.5 min before layer transfer was visually observed. Temperature profiles were monitored using a Raytek Compact MID series pyrometer. The resulting SOI surface quality was characterized using a Nanoscope IIIA atomic force microscope (AFM) in tapping mode in order to determine the root-mean-square (rms) roughness of the transferred layer. Rutherford backscattering (RBS) in both random and channeled orientations was performed using a 1.7 MV tandem accelerator. RUMP (Ref. 7) software was then used to simulate layer thicknesses and to evaluate the crystallinity of the transferred layer. Hall effect measurements were obtained to examine the electrical characteristics of the “as-exfoliated” samples. Cross-section transmission electron microscopy (TEM) was performed to examine microstruc-

^{a)}Electronic mail: alford@asu.edu

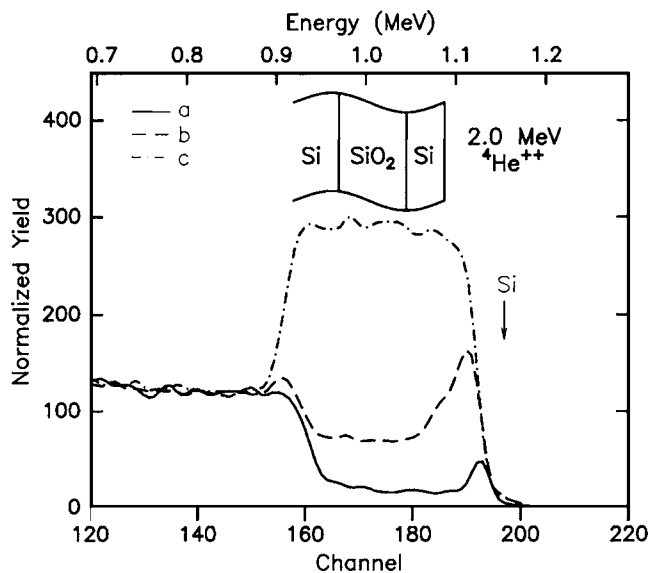


FIG. 1. RBS spectra obtained from a 470 nm thick silicon layer transferred using a microwave-initiated ion-cut process. (a) $\langle 100 \rangle$ aligned scattering from the transferred layer after damage repair by vacuum furnace annealing, (b) $\langle 100 \rangle$ aligned scattering from the transferred layer as cut, with no additional annealing, and (c) random nonaligned scattering from the as-cut layer.

ture and defect behavior in the transferred layers. After initial characterization, the samples were annealed in a vacuum carousel furnace with temperatures ranging from 600 °C to 800 °C, for time durations between 2 and 4 h at a pressure of 10^{-7} Torr. This was followed by electrical measurements, TEM, and RBS in order to characterize the repair of any radiation damage that may have been created in the ion-cut process.

Figure 1 presents RBS spectra obtained from random and channeled orientations of a typical transferred layer. Spectra from the transferred layer in both random and channeled orientations demonstrate that the ion-cut process was successful in using microwaves to initiate the exfoliation of single-crystal silicon.^{8,9} RUMP simulation of the RBS spectra (c) determined the thickness of the transferred layer to be 470 nm, and that of the oxide layer 725 nm. TRIM (Ref. 10) calculations demonstrated that the thickness of the exfoliated layer correlated well with the peak in the radiation damage caused by implantation, and not the projected ranges of the implant species. Projected ranges for the boron and hydrogen implants used in Fig. 1, determined using TRIM calculations, were approximately 512 nm and 452 nm, respectively. Spectrum (c), obtained from an “as-cut” sample in random orientation, indicates the presence of a continuous layer of silicon on top of the insulator; while also hinting at a mild surface microroughness as is evident from the width of the low-energy edge at channels 150–160.⁹ Spectrum (b), obtained from an $\langle 100 \rangle$ aligned sample of as-cut SOI, shows a dramatic decrease in yield, indicating that the transferred layers have kept their crystallinity. The width of the surface peak in the as-cut channeled spectrum (b) indicates that the majority of the radiation damage was concentrated at the top of the transferred layer. As can be seen when comparing channeled spectrum (a), obtained from an annealed transferred layer, and channeled spectrum (b), obtained from the as-cut transferred layer, most of the radiation damage was repaired upon further annealing of the microwave-initiated ion-cut samples.

TABLE I. Hall effect electrical measurements obtained from the silicon donor substrate and SOT transferred layer after microwave-initiated ion-cut exfoliation for SOI. The donor silicon was implanted with 9×10^{16} H⁺ions/cm² at 50 keV, and 2×10^{14} B⁺ions/cm² at 175 keV.

Category	Description	Resistivity (Ω cm)	Type	Concentration (cm ⁻³)	Mobility (cm ² /V s)
Donor Si	As exfoliated	3.88	<i>n</i>	1.3×10^{15} (cm ⁻²) ^a	57
SOI	As exfoliated	3.83	<i>n</i>	5.49×10^{16}	69
	500 °C, 2 h	4.2	<i>n</i>	6.2×10^{16}	24
	600 °C, 2 h	4.0	<i>p</i>	2.13×10^{17}	7
	700 °C, 2 h	0.0447	<i>p</i>	1.56×10^{18}	89
	700 °C, 4 h	0.0374	<i>p</i>	2.05×10^{18}	80
	800 °C, 2 h	0.023	<i>p</i>	3.32×10^{18}	82

^aSheet charge is reported because the damage layer thickness was not known exactly. The layer thickness can be estimated as $2R_p$, which would be approximately 1000 nm for this sample.

This finding compares well with previous ion-cut techniques.^{11,12}

AFM microroughness measurements taken across a one μm^2 sampling area demonstrated little variability in the rms roughness of the sample. Because the AFM measurements were obtained in tapping mode, they could be repeated, and averages used. The rms roughness of the sample averaged 5.3 nm. Depending on implantation parameters, incubation times, and anneal temperatures, previously documented microroughnesses vary between 3.4 nm and 10 nm over one micron sampling distances.^{2,9,11}

Table I displays changes in resistivity, dominant carrier species, carrier concentration, and electronic mobility as a function of anneal temperature and time for successive high-temperature anneals of a microwave-initiated exfoliated layer. The anneals were performed in order to repair radiation damage in the transferred layer. The high-temperature anneals were performed in a vacuum furnace instead of a microwave oven in order to have a common reference point for comparison with previous work.^{2,9,13} When viewing the data in Table I, most noteworthy is the change in conductivity type, and the temperature of the anneals where this change takes place. The observed trend compares well with previous work,^{2,9,13} in which the surface of uncut samples were *p* type, cut sample surfaces were *n* type, and upon successive anneals the cut sample surfaces returned to *p* type. The change in conductivity type upon exfoliation has been proposed as being due to hydrogen-related shallow donors and ion-enhanced diffusion of interstitial oxygen giving rise to thermal donors.¹² Published values of *p*-type mobility in unetched samples range from 9–121 cm²/V s.^{2,12,13} In previous papers, the carrier concentrations of samples measured after anneals above 650 °C were significantly lower ($\sim 10^{16}/\text{cm}^3$ – $10^{17}/\text{cm}^3$) than the results attained here; unfortunately, these papers did not have boron co-implants.^{2,9,13} The authors believe that the change in hole carrier concentration is explained by electrical activation of some of the co-implanted boron. The hole mobilities attained in this work compare well with mobilities attained in single-crystal silicon with the same carrier concentrations.¹⁴

Figure 2 presents cross-sectional TEM images of the transferred silicon layer in SOI samples that were created by the microwave-initiated ion-cut process. Micrographs of the samples (a) before and (b) after the anneals tabulated in Table I are shown. In Fig. 2(a), a damage-containing region

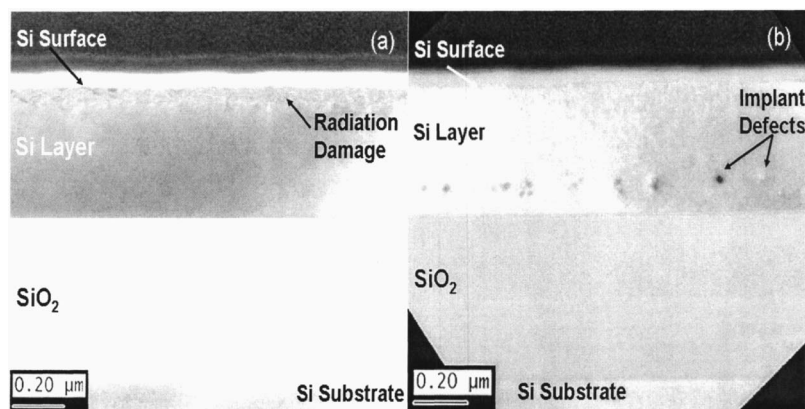


FIG. 2. Cross-sectional TEM micrographs showing (a) preanneal and (b) postanneal radiation damage in microwave-initiated ion-cut samples. The preanneal sample displays radiation damage at the top of the transferred layer. For these samples, 9×10^{16} H⁺ ions/cm² and 2×10^{14} B⁺ ions/cm² were co-implanted, at 50 keV and 175 keV energies, respectively.

is visible near the surface of the transferred layer. This damage is consistent with radiation damage from hydrogen and boron ions in the as-cut sample. Prior to any anneals, the majority of the radiation damage is present at the surface of the transferred layer, and the damage region encompasses approximately 25%, or 120 nm, of the total layer thickness. TRIM calculations for the boron implants of the sample in Fig. 2 yield a ΔR_p value of approximately 100 nm. For the given concentrations and energies of hydrogen and boron ions irradiating the sample, these results are consistent with previous papers.^{9,12,13,15} As can be seen in Fig. 2(b), after sequential anneals to repair radiation damage, there is little to no visible damage near the surface of the transferred layer. The only visible damage appears near the bottom of the transferred layer. This damage can be accounted for as dislocation loops created during the sequential high-temperature anneals of the sample. Intrinsic dislocation loops are created during postimplantation annealing, when shallow level vacancies, which accompany deep-level interstitials, coagulate.

Unlike traditional heating, the implanted species (H⁺ and B⁺) involved in ion cutting serve to increase the rapid heating of silicon by microwaves because implanted boron and hydrogen create complex dipoles and charge states which contribute to the samples effective dielectric loss and ionic conduction.^{16,17} Power absorption in microwave heating is volumetric and is directly proportional to the samples' dielectric loss and ionic conduction.¹⁸ The increased damage in the silicon, resulting from the ion implantation, serves to increase power absorption during microwave heating. This is a significant and beneficial side effect of creating radiation damage in ion-cut samples. Furthermore, the silicon itself absorbs microwave power volumetrically, increasing damage and platelet size in the ion-cut region from within the bonded layer instead of through convection or conduction used in normal heating processes. The authors suspect that this increased local power absorption, combined with volumetric heating, is what shortens the incubation time in the case of microwave heating, as compared with traditional ion-cut heating processes.

Although the microwave initiation of ion cutting took place in as little as 12 s, the temperatures of the samples at the time of the exfoliation were between 300 °C–425 °C depending on process time, similar to other ion-cut processes.^{9,13,15} Aside from the increased speed in processing, the significant differences between “microwave cutting”

and conventional heating are: The greater power efficiency of microwave magnetron generators in comparison to resistance heating in furnaces, the volumetric heating associated with microwave heating, and the possibility of tailoring the sample temperature based on the resistivity of the transferred silicon and silicon substrate material. The ability to tailor sample temperatures based on material properties opens new possibilities for the creation of heterogeneous structures using the ion-cut process.

This work was partially supported by a grant from the NSF (DMR-0308127, L. Hess), and a Strategic Research Grant from City University of Hong Kong (SRG No. 7001820). The work at Los Alamos National Laboratory was supported by the DOE Office of Basic Energy Sciences.

¹C. Maleville and C. Mazure, *Solid-State Electron.* **48**, 1055 (2004).

²F. Lu, D. Qiao, M. Cai, P. K. L. Yu, S. S. Lau, R. K. Y. Fu, L. S. Hung, C. P. Li, P. K. Chu, H. C. Chein, and Y. Liou, *J. Vac. Sci. Technol. B* **21**, 2109 (2003).

³R. Subasri, T. Matthews, O. M. Sreedharan, and V. S. Ragunathan, *Solid State Ionics* **158**, 199 (2003).

⁴R. Roy, D. Agrawal, J. Cheng, and S. Gedevarishvili, *Nature (London)* **399**, 668 (1999).

⁵S. Aravindan and R. Krishnamurthy, *Ceram. Trans.* **111**, 287 (2001).

⁶D. C. Thompson, H. C. Kim, T. L. Alford, and J. W. Mayer, *Appl. Phys. Lett.* **83**, 3918 (2003).

⁷L. R. Doolittle, *Nucl. Instrum. Methods Phys. Res. B* **9**, 344 (1985).

⁸T. Hochbauer, A. Misra, M. Nastasi, K. Hentinen, T. Suni, I. Suni, S. S. Lau, and W. Ensinger, *Nucl. Instrum. Methods Phys. Res. B* **216**, 257 (2004).

⁹J. K. Lee, M. Nastasi, N. D. Theodore, A. Smalley, T. L. Alford, J. W. Mayer, M. Cai, and S. S. Lau, *J. Appl. Phys.* **96**, 280 (2004).

¹⁰J. F. Zeigler, IBM Research, Yorktown, NY, 10598.

¹¹J. Du, W. H. Ko, and D. J. Young, *Sens. Actuators, A* **112**, 116 (2004).

¹²V. P. Popov, I. V. Antonova, V. F. Stas, L. V. Mironova, A. K. Gutakovskii, E. V. Spesivtev, A. S. Mardegzoh, A. A. Franzusov, and G. N. Feofanov, *Mater. Sci. Eng., B* **73**, 82 (2000).

¹³M. Cai, D. Qiao, L. S. Yu, S. S. Lau, C. P. Li, L. S. Hung, T. E. Haynes, K. Hentinen, I. Suni, V. M. C. Poon, T. Marek, and J. W. Mayer, *J. Appl. Phys.* **92**, 3388 (2002).

¹⁴R. F. Pierret, *Semiconductor Device Fundamentals* (Addison-Wesley, Reading, MA, 1996), p. 80.

¹⁵Q.-Y. Tong, R. Scholz, U. Gosele, T.-H. Lee, L.-J. Huang, Y.-L. Chao, and T. Y. Tan, *Appl. Phys. Lett.* **72**, 49 (1998).

¹⁶S. J. Pearton, J. W. Corbett, and M. Stavola, *Hydrogen in Crystalline Semiconductors* (Springer, New York, 1992).

¹⁷J. T. Borenstein, J. W. Corbett, and S. J. Pearton, *J. Appl. Phys.* **73**, 2751 (1993).

¹⁸B. Meng, B. D. B. Klein, J. H. Booske, and R. F. Cooper, *Phys. Rev. B* **53**, 12777 (1996).